



Numerical Modeling of Effects of Excitons on Photoelectric Properties of Cells

Modou Faye^{1*}, Mamadou Niane¹, Saliou Ndiaye¹, Ousmane Ngom¹, Cheikh Mbow², Bassirou Ba¹

^{1*}Department de Physique, Faculté des Sciences et Techniques, Laboratoires des Semiconducteurs et d'énergie Solaire, Université Cheikh Anta Diop, Dakar, Sénégal.

²Department de Physique, Faculté des Sciences et Techniques, Laboratoire de Mécanique des Fluides, Hydraulique et Transferts, Université Cheikh Anta Diop, Dakar, Sénégal

Abstract In this study, we analyze numerically the exciton effects on the density of photocurrent, generated by a semiconductor. The semiconductor contains electrons and excitons. The generation of the latter depends on absorption and the average temperature. This absorption can be dominated by the electrons ($f_e = 1$) or by excitons ($f_x = 1$). The dependence of the total density of photocurrent compared to the temperature or of absorption characterizes each type of distribution of the carriers. It is then significant to know the nature of the dependence of the total density of photocurrent according to absorption and of the temperature for each type of distribution of carriers. In addition, we are in front of a non-linear problem. For the numerical resolution of such a problem, we chose the method of finished volumes. The system of algebraic equations obtained is solved grace to the method of double course combined with an iterative method of relieving line by line of the Gauss-Seidel type.

Keywords Excitons, Absorption, Numbers of Fourier, Heating factor

1. Introduction

A exciton is a quasi-particle noncharged, formed with a bound electron-hole pair by a Coulomb interaction. This strongly dependent electron-hole pair is created by the absorption of the photons by the cell. Indeed, excitons are mobile, electrically neutral and strongly localized. Their participation in the total density of photocurrent in material, results from the difference between the number of generations of electron-hole pairs and the number of recombinations. This difference grows with the rise in the temperature.

In order to increase the output and to reduce the manufacturing cost of the solar cells, the researchers always directed themselves towards the inorganic semiconductors at base of silicon. Certain authors like, Mr. Burgelman and B Minnaer [2] developed a digital model applicable to the solar cells in the presence of excitons. They showed that the concentration of excitons can approach that of the electrons.

The objective of our study is to develop a digital model applicable to the inorganic solar cells including excitons for various values wavelength and absorption coefficient. We carried out it by considering a solar cell subjected to a monochromatic illumination through the front face and a heat insulation by the back face by taking account of the inclusion of the space charge layer. We have considered the non-uniformity of dissociation and the recombination of excitons in this space. The simultaneous taking into account of the variability of the coefficients according to the temperature and the presence of the electric field in the space charge layer is a first in this kind of study. Consequently, we are in front of a non-linear physical problem, very complex. Any analytical solution is impossible. This is why our choices were made on the mathematical and numerical models.



2. Position of the problem and mathematical formulation

2.1. Physical position of the problem and Assumptions

We will consider a semiconductor length L (figure 1), in one dimensional matter, areas with no-homogeneous doping. We admit that the electric field in the space charge layer is a linear function of the X-coordinate z which one can put in the form:

$$E(z) = \frac{E_m}{w}(w - z) \text{ and } b(z) = b[E(z)] \text{ in } (0 \leq z \leq w)$$

We took account also of the absorption due of the electron-hole pairs such as $f_e + f_x = 1$ [2]. With f_e is the fraction of electrons and f_x is that of excitons.

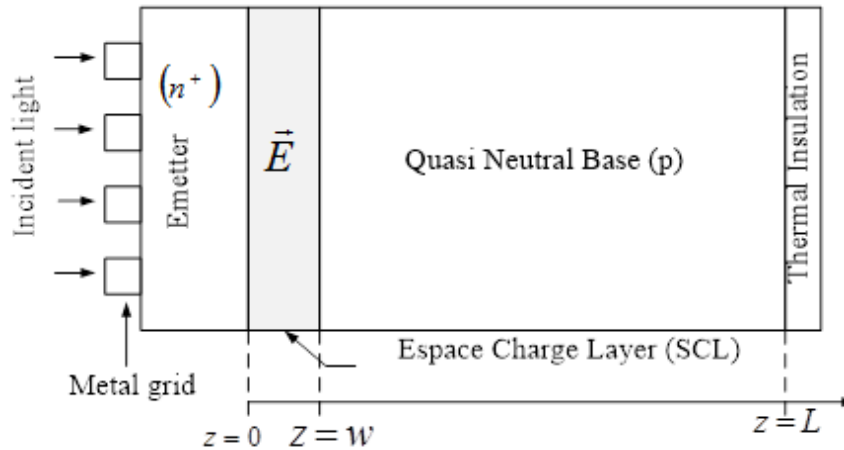


Figure 1: Schematics of a semiconductor to silicon n⁺p-junction.

In more we suppose the faces $z = 0$ and $z = L$ are the seat of phenomena of recombinations in volume and the surface.

The diffusion of the electrons and excitons coefficients are related to certain variables, in particular the temperature of material. They are given by the relation of Einstein [12].

2.2. Mathematical formulation

Taking into account the assumptions of modeling above and the physical sizes of reference following: C_r ,

(concentration for the electrons), $\Delta T_r = \frac{q_m \times L}{\lambda}$ (for the variation in temperature), L and W (for the space

variable z), G_r (rate of generation of the electrons and excitons). The adimensional expressions defined by the reference variables are:

$$z^* = \frac{z}{L}, z^* = \frac{w}{L}, n_e^* = \frac{n_e}{C_r}, n_h^* = \frac{n_h}{C_r}, n_x^* = \frac{n_x}{C_r}, n_{in}^* = \frac{n_{in}}{C_r},$$

$$G^* = \frac{G_{eh}}{G_r}, G^* = \frac{G_x}{G_r}, t^* = \frac{a}{L^2} t, T^* = \frac{T - T_a}{\Delta T_r}$$

The carriers generation rates are given by [4]:

$$G_{eh} = G_{eho} \exp(-\alpha z) ; G_x = G_{xo} \exp(-\alpha z)$$

With

$$G_{eho} = f_e \alpha(\lambda) N(\lambda) ; G_{xo} = f_x \alpha(\lambda) N(\lambda)$$

$$N(\lambda) = 5.03110^{+18} \lambda P(\lambda)$$

$$\alpha(\lambda) = 0.526367 - 1.14425 / \lambda + 0.585368 / \lambda^2 + 0.039958 / \lambda^3$$



Where: λ the illumination wavelength;

$\alpha(\lambda)$ the absorption coefficient.

The a dimensional equations of a coupled system and that of heat become:

$$F_{e0} \frac{\partial}{\partial z^*} \left\{ D_T^* \frac{\partial n_e^*}{\partial z^*} \right\} + A \frac{\partial}{\partial z^*} \left\{ n_e^* (w^* - z^*) \right\} = \frac{n_e^* n_h^* - n_{in}^{*2}}{n_e^* + n_h^* + 2n_{in}^*} + B_e (n_e^* n_h^* - n_x^* n_1^*) - C_e f_e G^* \tag{1a}$$

$$F_{x0} \frac{\partial}{\partial z^*} \left\{ R_\mu D_T^* \frac{\partial n_x^*}{\partial z^*} \right\} = (n_x^* - n_{x0}^*) - B_x (n_e^* n_h^* - n_x^* n_1^*) - C_x (1 - f_e) G^* \tag{1b}$$

$$\frac{\partial T^*}{\partial z^*} = \frac{\partial^2 T^*}{\partial z^{*2}} \tag{2}$$

The expressions of the characteristic numbers are:

$$A = \frac{\mu_e \tau_e E_m}{w} ; A_{eL} = \frac{D^0}{LS_e} ; A_{xL} = \frac{D^0}{LS_x} ; A_{0x} = \frac{D^0}{LS_{0x}} ; B_{eL} = \frac{b_s}{S_e} ; B_{xL} = \frac{b_s}{S_x} ; B_{0x} = \frac{b_s}{S_{0x}} ;$$

$$B_e = \tau_e b C_r ; B_x = \tau_x b C_r ; C_e = \frac{\tau_e G_r}{C_r} ; C_x = \frac{\tau_x G_r}{C_r}$$

And the characteristic a dimensional numbers are:

$$F_0 = \frac{\tau \times D^0}{L^2} \quad \text{Relationship between the time of diffusion and the lifespan (a number of Fourier).}$$

$$R_\mu = \frac{\mu_x}{\mu_e} \quad \text{Relationship between the mobility of excitons and electrons.}$$

The quantity D^0 is the diffusion of the electrons coefficient calculated starting from the ambient temperature T_a considered as constant. The "diffusion coefficient" a dimensional D_T^* expression is:

$$D_T^* = 1 + \frac{\Delta T_r}{T_a} T^* \tag{3}$$

It is thus a function of the a dimensional temperature T^* . The quantity $Fact - ch = \frac{\Delta T_r}{T_a}$ is called heating

factor. It is the relationship between the imposed conduction and heat flows. To supplement the system (1)-(2) in the interval $[0,1]$, we associate to him the initial conditions and of the boundary conditions a dimensional. Their expressions are consigned in table 1 below:

Table 1: Initial and boundary conditions associated of the dimensionless electrons, excitons and the temperature

For the electrons	For the excitons
$z^* = 0 \Rightarrow n_e^*(0) = N_D^*$	$z^* = 0 \Rightarrow A_{0x} \frac{\partial}{\partial z^*} \{ R_\mu D_T^* n_x^* \}_{z=0} = [n_x^*(0) - n_{x0}^*] - B_{0x} [n_x^*(0) - n_{x1}^*]$
$z^* = 1 \Rightarrow A_{Le} \frac{\partial}{\partial z^*} \{ D_T^* n_e^* \}_{z=1} = -[n_e^*(1) - n_{e0}^*] + B_{Le} [n_x^*(1) - n_{x1}^*]$	$z^* = 1 \Rightarrow A_{Lx} \frac{\partial}{\partial z^*} \{ R_\mu D_T^* n_x^* \}_{z=1} = -[n_x^*(1) - n_{x0}^*] - B_{Lx} [n_x^*(1) - n_{x1}^*]$
Conditions on the temperature	
$t^* = 0 \Rightarrow T^*(z^*, 0) = 0$	
$z^* = 0 \Rightarrow \frac{\partial T^*}{\partial z^*} = -g(t^*)$	
$z^* = 1 \Rightarrow \frac{\partial T^*}{\partial z^*} = 0$	



3. Numerical Procedure

These a dimensional equations very complex, that is to say non-linear on the one hand and are coupled on the other hand. In this case, the recourse to the numerical resolution is essential and incites us to choose the adequate numerical method to obtain the best approximations.

In what concerns us, we chose the method of finished volumes, because it has considerable advantages owing to the fact that it is simple, that it facilitates the linearization of the sources terms if they are not it and allows an easier processing of the heterogeneous mediums.

As the various areas of our field (the space charge layer and the base) are not same dimensions and are the seat of physical phenomena of very different nature it is advisable to use a variable grid. The distributions of the electrons and the excitons being very sensitive to the phenomena of surface a fine grid in the vicinity of $z = 0$ and of $z = 1$ is adopted. However, the fact of taking a very fine grid can lead paradoxically to results deprived of physical direction because of the accumulation of the errors of machine. This is why we thus used grid of the trigonometrical type.

The principle of the method of finished volumes consists in integrating the transport equations on a discrete whole of jointed finished volumes, called volumes of control, thus covering all the physical field [5].

The system of algebraic equations obtained is solved thanks to the method of double course combined with an iterative method of relieving line by line of the Gauss-Seidel type.

$$(B_0 \delta z_1 - A_0 D_k) \phi_{k,1} + A_0 D_k \phi_{k,2} = (D_0 - C_0 \phi_{l,1}) \delta z_1 \quad i = 1 \quad (4a)$$

$$-a_{N,k} \phi_{k,i-1} + a'_{M,k} - a_{p,k} \phi_{k,i+1} = S'_{m,k} \quad 1 < i < i_m \quad (4b)$$

$$-A_1 D_k \phi_{k,i_{m-1}} + (B_1 \delta z_{i_{m-1}} + A_1 D_k) \phi_{k,i_m} = (D_1 - C_1 \phi_{l,i_m}) \delta z_{i_{m-1}} \quad i = i_m \quad (4c)$$

4. Results and Discussion

The results resulting from mathematical and numerical modeling of the various phenomena are summarized by considering the representation hereafter.

We present primarily the influences of the fraction of the carriers, of the number of Fourier and the heating factor on the total density of photocurrent of the electrons and excitons in the junction.

The tests which we carried out showed that the step of time, the index who locates the position of the interface zone of load of espace/base, the number of nodes, the allowed relative error and the parameter of relieving $\delta t^* = 10^{-3}$; $i_w = 81$; $i_m = 201$; $\varepsilon = 10^{-3}$ and $w = 0.15$ is good compromises between an acceptable computational load and a reasonable calculating time. The voluminal coefficient of coupling which depends on the average temperature is given by $bv = (10^{-2} \times T_{moy}^{-2} + 2.5 \times 10^{-6} \times T_{moy}^{-0.5} + 1.5 \times 10^{-7})$ [4]. With T_{moy} the average temperature.

In this part, we will study the effects of the fraction of the carriers, of the number of Fourier and the heating factor on the total density of photocurrent of the electrons and excitons according to the wavelength and possibly the absorption coefficient. The expressions of the total density of photocurrent are given in [6].

4.1. Influence of the fraction of carriers

The curves of figures 2, 3 and 4, show that, for $f_x = 1$ the total density of photocurrent is weak and it remains constant for the various values wavelength and absorption coefficient. In addition, the total density of photocurrent starts to increase for $f_e = 0.5$ and $f_x = 0.5$, that is to say if a half is absorbed the electrons and another half by excitons. This increase is more significant, when we are in the case of the inorganic semiconductors, that is to say for $f_e = 1$ and $f_x = 0$. This is still explained by the fact why, the mathematical model that we developed is applicable to the inorganic semiconductors.

For the wavelengths higher than $1.05 \mu\text{m}$ approximately, the photocurrent decreases. This reduction is due to the fact that there are less photo carriers generated for the big wavelengths. Whereas, in this range big wavelengths, the total density of photocurrent (figures 3b and 4b) increases according to the absorption coefficient. This



shows the non-linearity of our physical problem due to the voluminal coefficient of coupling and the rate of recombination given by the formula of Shockley-Read [2].

The results obtained with an illumination by the front face show that we have the same analyses as with those obtained with the face subjected to a thermal insulation. Lastly, the influence of absorption due to the electron-hole pairs, with each fixed value, the total density of photocurrent varies for the various values wavelength and absorption coefficient.

For the face subjected to a heat insulation, the noted values of the total density of photocurrent (figures 2b and 4) are higher than those obtained for an illumination by the front face (figures 2a and 3). These observations are explained by the fact why, on the one hand, the photo carriers created by the back face migrate towards the junction with less losses by recombination in volume and on the other hand the participation of excitons with the total density of photocurrent. Consequently, there will be more carriers which will cross the junction and will contribute to the photocurrent.

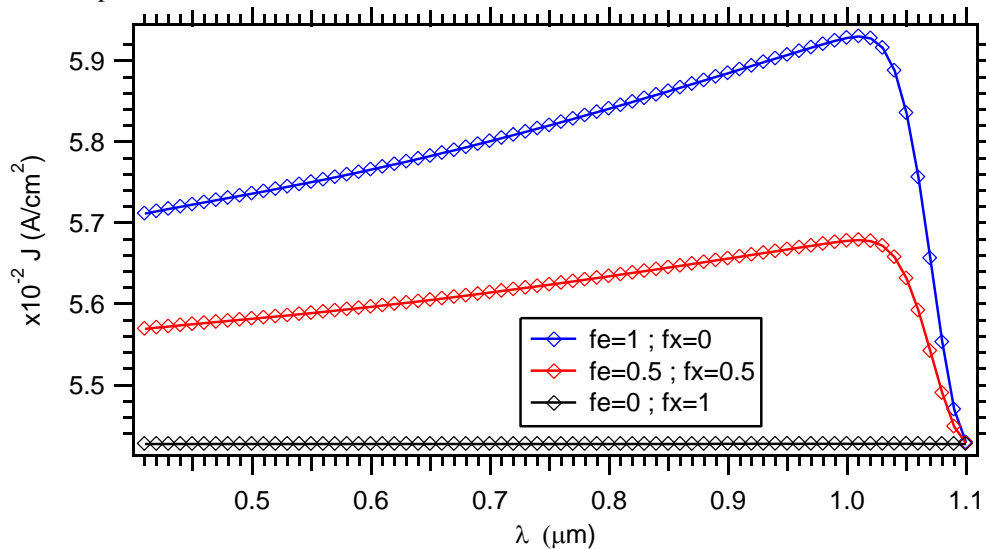


Figure 2a: Influence of the fraction on the variation of the total density of photocurrent of the charge carriers according to the wavelength $N_A=10^{16} \text{ cm}^{-3}$; $N_D=10^{19} \text{ cm}^{-3}$; $n_i=1,45 \cdot 10^{10} \text{ cm}^{-3}$; $n_{\text{mott}}=1,0310^{18} \text{ cm}^{-3}$; $bs=10^{-2} \text{ cm s}^{-1}$; $Se= Sx=10 \text{ cm s}^{-1}$; $Fo=10$; $\text{Fact}_{\text{ch}}=2 \times 10^{-2}$

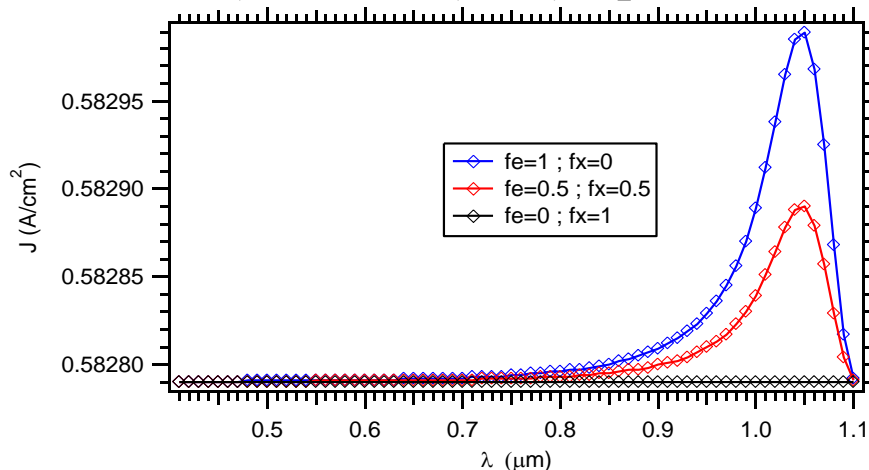


Figure 2b: Influence of the fraction on the variation of the total density of photocurrent of the charge carriers according to the wavelength: face subjected to a heat insulation $N_A=10^{16} \text{ cm}^{-3}$; $N_D=10^{19} \text{ cm}^{-3}$; $n_i=1,45 \cdot 10^{10} \text{ cm}^{-3}$; $n_{\text{mott}}=1,0310^{18} \text{ cm}^{-3}$; $bs=10^{-2} \text{ cm s}^{-1}$; $Se= Sx=10 \text{ cm s}^{-1}$; $Fo=10$; $\text{Fact}_{\text{ch}}=2 \times 10^{-2}$

The figures 2a and 2b above, show that, to see the effects of volume and those of surface we can continue our simulation with the great values length.



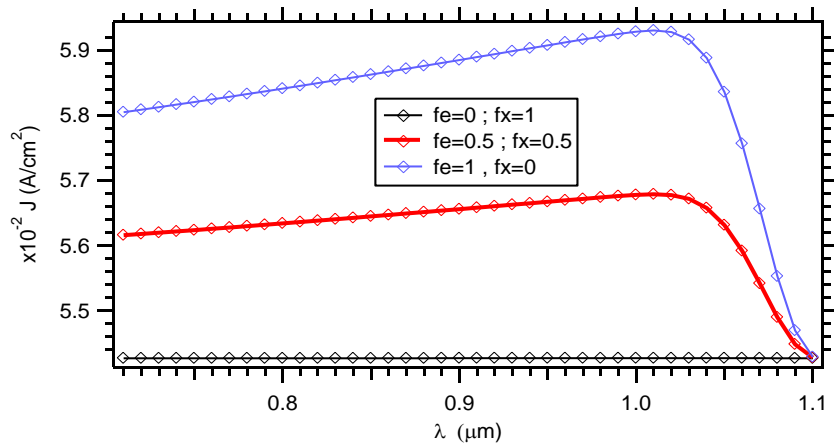


Figure 3a: Influence of the fraction on the variation of the total density of photocurrent of the charge carriers according to the wavelength
 $N_A=10^{16} \text{ cm}^{-3}$; $N_D=10^{19} \text{ cm}^{-3}$; $n_i=1,45 \cdot 10^{10} \text{ cm}^{-3}$; $n_{\text{mott}}=1,0310^{18} \text{ cm}^{-3}$; $bs=10^{-2} \text{ cm s}^{-1}$; $Se= Sx =10 \text{ cm s}^{-1}$;
 $Fo=10$; $Fact_{\text{ch}}=2 \times 10^{-2}$

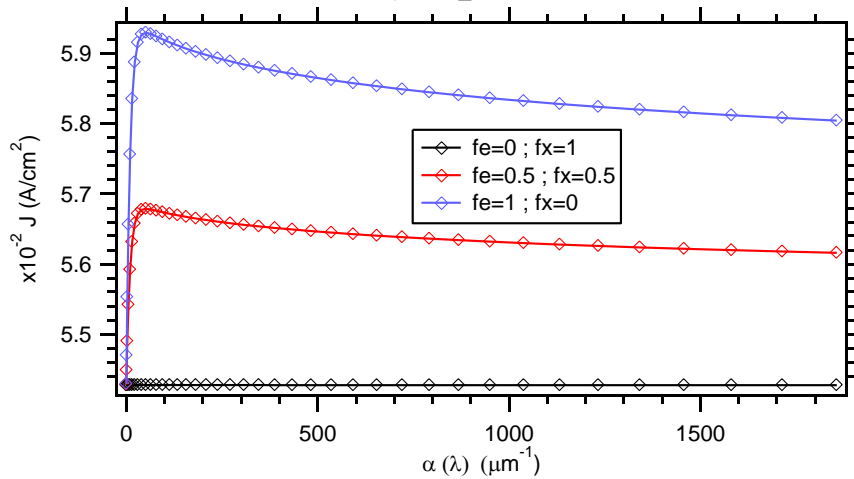


Figure 3b: Influence of the fraction on the variation of the total density of photocurrent of the charge carriers according to the absorption coefficient
 $N_A=10^{16} \text{ cm}^{-3}$; $N_D=10^{19} \text{ cm}^{-3}$; $n_i=1,45 \cdot 10^{10} \text{ cm}^{-3}$; $n_{\text{mott}}=1,0310^{18} \text{ cm}^{-3}$; $bs=10^{-2} \text{ cm s}^{-1}$; $Se= Sx =10 \text{ cm s}^{-1}$;
 $Fo=10$; $Fact_{\text{ch}}=2 \times 10^{-2}$

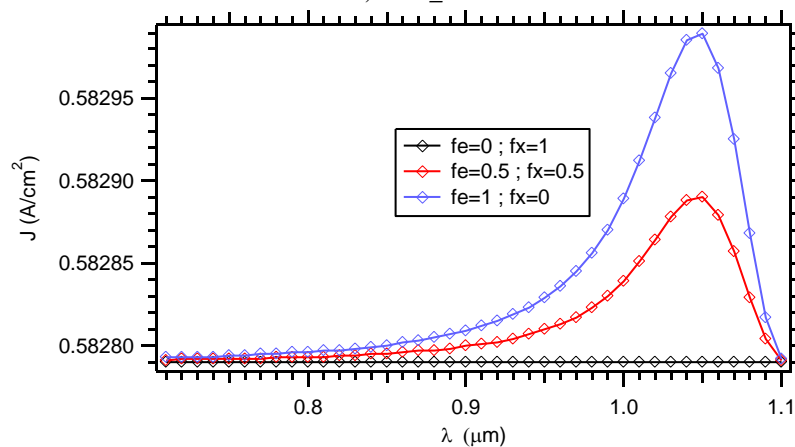


Figure 4a: Influence of the fraction on the variation of the total density of photocurrent of the charge carriers according to the wavelength: face subjected to a heat insulation
 $N_A=10^{16} \text{ cm}^{-3}$; $N_D=10^{19} \text{ cm}^{-3}$; $n_i=1,45 \cdot 10^{10} \text{ cm}^{-3}$; $n_{\text{mott}}=1,0310^{18} \text{ cm}^{-3}$; $bs=10^{-2} \text{ cm s}^{-1}$; $Se= Sx =10 \text{ cm s}^{-1}$;
 $Fo=10$; $Fact_{\text{ch}}=2 \times 10^{-2}$

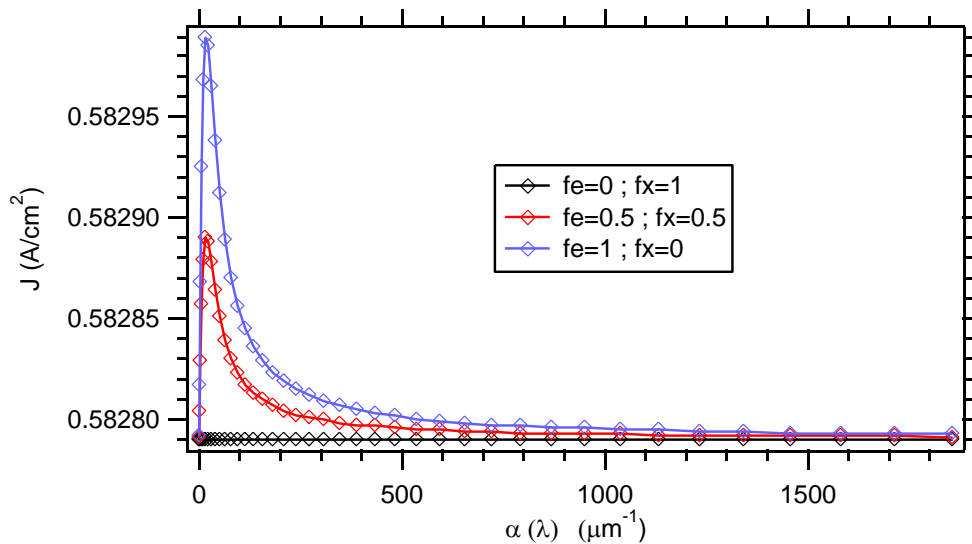


Figure 4b: Influence of the fraction on the variation of the total density of photocurrent of the charge carriers according to the absorption coefficient: face subjected to a heat insulation
 $N_A=10^{16} \text{ cm}^{-3}$; $N_D=10^{19} \text{ cm}^{-3}$; $n_i=1,45 \cdot 10^{10} \text{ cm}^{-3}$; $n_{\text{mott}}=1,0310^{18} \text{ cm}^{-3}$; $bs=10^{-2} \text{ cm s}^{-1}$; $Se= Sx =10 \text{ cm s}^{-1}$;
 $Fo=10$; $Fact_{\text{ch}}=2 \times 10^{-2}$

In the continuation of the study of the total density of photocurrent, calculated for various values length or absorption coefficient, we considered the case where $f_e = 1$ that is to say of an inorganic semiconductor.

To minimize the effects the big wavelengths on the number of generated photo carriers and the absorption dominated by excitons ($f_x = 1$), we continue our simulation with the influences of the number of Fourier and the heating factor.

4.2. Influences of the number Fourier and the heating factor.

By taking account of all the observations and preceding explanations, we can add that the number of Fourier (figure 5a) and the heating factor (figure 5b) have each one a considerable effect on the variation of the total density of photocurrent according to the wavelength. The increase in the latter entraine that of the total density of photocurrent because the excited carriers arrive at the junction. Moreover, in the range big wavelengths, the number of Fourier and the heating factor reduce the reduction in the total density of photocurrent. Consequently, they support the total packing of photocurrent.

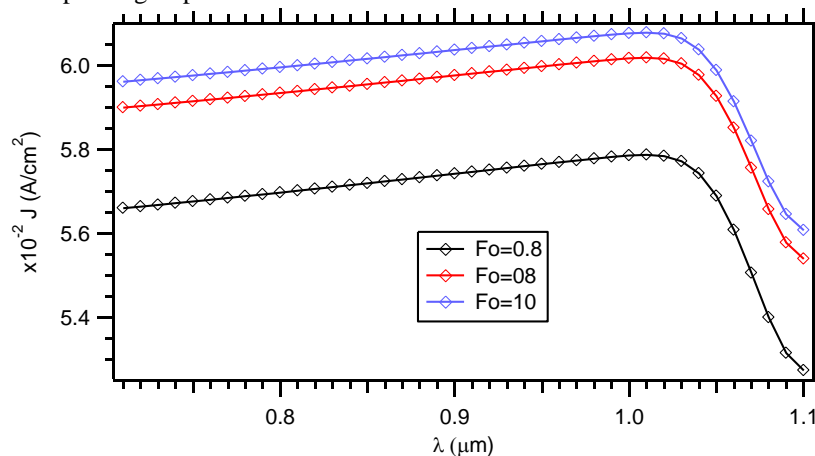


Figure 5a: Influence of the number of Fourier on the variation of the total density of photocurrent of the charge carriers according to the wavelength
 $N_A=10^{16} \text{ cm}^{-3}$; $N_D=10^{19} \text{ cm}^{-3}$; $n_i=1,45 \cdot 10^{10} \text{ cm}^{-3}$; $n_{\text{mott}}=1,0310^{18} \text{ cm}^{-3}$; $bs=10^{-2} \text{ cm s}^{-1}$; $Se= Sx =10 \text{ cm s}^{-1}$;
 $Fact_{\text{ch}}=2 \times 10^{-2}$



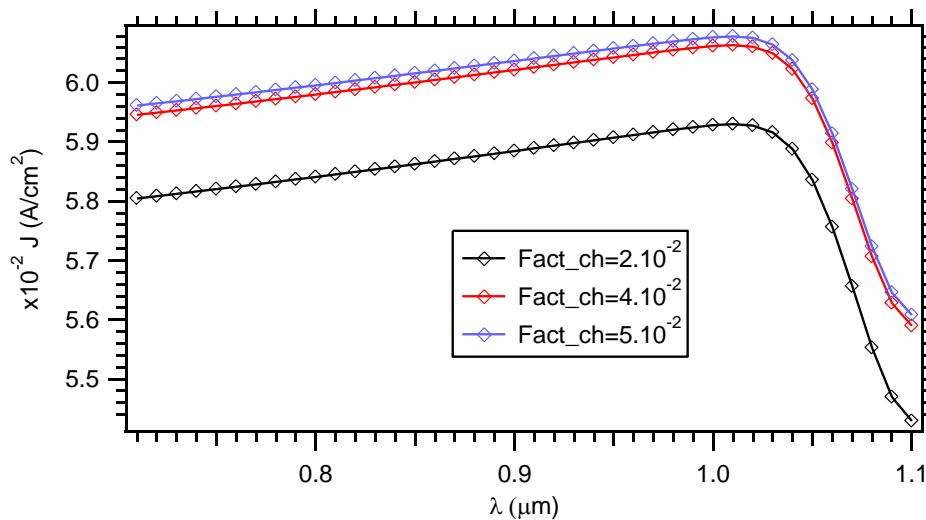


Figure 5b: Influence of the heating factor on the variation of the density of photocurrent of the load carriers according to the wavelength

$$N_A=10^{16} \text{ cm}^{-3}; N_D=10^{19} \text{ cm}^{-3}; n_i=1,45 \cdot 10^{10} \text{ cm}^{-3}; n_{\text{mott}}=1,03 \cdot 10^{18} \text{ cm}^{-3}; b_s=10^{-2} \text{ cm s}^{-1}; S_e=S_x=10 \text{ cm s}^{-1}; Fo=10$$

5. Conclusion

The numerical study of the exciton effects on the photoelectric properties in an inorganic semiconductor led us to the following results: The strong coupling or the non-linearity of the physical problem is mainly at the origin of the analytical resolutions never realized. It is for that, the use of the method of finished volumes proves to be essential to discretize the transport equations of charge carriers and that of heat. The algorithm of Thomas was used to solve them. The influence of the fraction of the carriers on the total density of photocurrent enabled us to conclude that our mathematical model is applicable to the inorganic semiconductors. It comes out from our study that we have the contribution of excitons on the total density of photocurrent with subjected to a heat insulation. The introduction of the number of Fourier and the heating factor have positive effects on the total density of photocurrent of the charge carriers. These two parameters reduced the negative effect of the great values wavelength on the total density of photocurrent.

References

- [1]. Kane, D. E.; Swanson, R. M. J. (1993). The effects of excitons on apparent band gap narrowing and transport in semiconductors. *Appl. Phys.*, 73, 1193-1197.
- [2]. Burgelman, M.; Minnaert, B. (2006). Including excitons in semiconductor solar cell modelling. *Thin Solid Films*, 511-512, pp 214-218.
- [3]. Karazhanov, S. Zh. (2000). Temperature and doping level dependence of solar cell performance including excitons. *Solar Energy Materials & Solar Cells*, 63, pp 149-163.
- [4]. Corkish, R.; Chan, D. S. P.; and Green, M. A. (1996). Excitons in silicon diodes and solar cells: A three-particle theory. *American Institute of Physics*, S0021-8979, 0070-9, pp 195-203
- [5]. Faye, M.; MBow, C.; Ba, B. (August 2014). Numerical Modeling of the Effects of Excitons in a Solar Cell Junction n⁺p of the Model by Extending the Space Charge Layer. *International Review of Physics (I.RE.PHY)*, ISSN 1971-680X. Vol. 8, N. 4, pp 102-109.
- [6]. Faye, M.; MBow, C.; Ba, B. (Feb - Mar. 2015). Development a Numerical Model Applicable to Inorganic and Organic Solar Cells Based on Silicon in the Presence of Excitons. *Current Trends in Technology and Science*, ISSN: 2279-0535. Volume: 04, Issue: 02, pp 491-497.
- [7]. Zhang, Y; Mascarenhas, A; Deb, S. (1998). Effects of excitons in solar cells. *J. Appl. Phys.*, 84, 3966-3971, 3966.



- [8]. Liang, Chunjun; Wang, Yongsheng; Li, Dan; Ji, Xingchen; Zhang, Fujun He, Zhiquan. (2014). Modelind and simulation of bulk heterojunction polymer solar cells. *Solar Energy Materials & Solar Cells* 127 67-86.
- [9]. Trukhanov, V. A; Bruevich, V.V; Paraschuk, D. Yu. (Dated: December 1, 2011). Effect of doping on performance of organic solar cells. International Laser Center and Faculty of Physics, M.V. Lomonosov Moscow State University, Moscow119991, Russia.
- [10]. Ji-Ting, Shieh; Chiou-Hua, Liu; Hsin-Fei, Meng; Shin-Rong, Tseng; Yu-Chiang, Chao; Sheng-Fu, Horng. (2010). The effect of carrier mobility in organic solar cells. *Journal of Applied Physics* 107, 084503.
- [11]. Patankar, S.V. “Numerical Heat Transfer and Fluid Flow”, Hemisphere Publishing Corporation, McGraw-Hill Book Company, 1981.
- [12]. Bird, R. B.; Stewart, W. E.; Lightfoot, E N. *Transport Phenomena*, John Wiley and Sons, Inc, New York 2001.
- [13]. Peaceman, D. W.; Rachford, H. A. The Numerical Solution of Parabolic and Elliptic Difference Equations, *J. Soc. Ind., Appli. Math*, 3, 28-43, 1955.

